Computers and Fluids 161 (2018) 23–32

Contents lists available at ScienceDirect

Computers and Fluids

journal homepage: www.elsevier.com/locate/compfluid

On the consequences of successively repeated collisions in no-time-counter collision scheme in DSMC

Hassan Akhlaghi[a], Ehsan Roohi[b,*], Stefan Stefanov[c]

[a] Aviation Technology Research Institute, Ferdowsi University of Mashhad, P.O. Box: 91779-48974, Mashhad, Iran
[b] High Performance Computing (HPC) Laboratory, Department of Mechanical Engineering, Ferdowsi University of Mashhad, P.O. Box: 91775-1111, Mashhad, Iran
[c] Institute of Mechanics, Bulgarian Academy of Science, Acad. G. Bontchev Str., 1113, Sofia, Bulgaria

ARTICLE INFO

Article history:
Received 1 July 2017
Revised 1 October 2017
Accepted 10 November 2017
Available online 11 November 2017

Keywords:
Collision-pair selection scheme
Fourier heat transfer problem
Successive duplicated collisions
Collisional parameters

ABSTRACT

The current paper investigates the appropriateness and consequences of avoiding successively repeated collisions usually recommended in the Direct Simulation Monte Carlo (DSMC) solvers, which use the No Time Counter (NTC) collision technique. A sensitive test case, i.e., Fourier heat transfer problem at the early slip regime, is considered in the presence and absence of the successively repeated collisions. The effects of repeated collisions and avoiding them on different parameters such as heat flux, collision frequency, collision separation distance, accepted-to-selected collisions ratio, and probability distribution functions for the number of collisions and relative velocities of collision pairs are evaluated and discussed. The investigations are performed considering contributions of different computational parameters, i.e., cell sizes, time step, and number of particles. In addition to collision frequency and collision separation distance, which were reported previously as crucial parameters affecting the accuracy of the DSMC solution, we found that the level of repeated collisions also plays a pivotal role in the accuracy of the heat flux prediction in the Fourier problem. We show that direct avoiding of repeated collisions can lead to a distortion of collision probability distribution and consequently, to introduction of a systematic error in collision frequency and predicted heat flux. This error is negligible if one uses a large number of particles per cell, but it is of considerable importance if there are a few particles per cell.

1. Introduction

Direct Simulation Monte Carlo (DSMC) can be considered as a numerical tool for solving the Boltzmann or Kac master equation based on the direct statistical simulation of the molecular processes described by the kinetic theory. The stochastic binary collision scheme plays a major role in the DSMC method. In the algorithms of most popular DSMC schemes the collision process could be divided into four steps, i.e., 1) determination of number of collision pairs or collision frequency estimate, 2) collision-pair selection, 3) acceptance-rejection process based on the collision probability function, and 4) determination of post-collision velocities for the accepted pair.

The Bird's No Time Counter (NTC) scheme has been widely adopted as the most commonly used collision scheme in DSMC. Due to the random selection of collision pairs, one of the main shortcomings of the standard NTC is the possibility of repeated collisions, i.e., the same pair of particles could repeatedly be selected for collision within one or several successive time steps without the occurrence of events of collisions with other particles [1]. Hence, NTC scheme requires a suitable number of particles in the cell to reduce the chance of successively repeated collisions. An insufficient number of particles per cell along with inappropriate temporal and spatial discretization are sources of stochastic errors, which violate the accuracy of the binary collision procedure [2–4]. Usually, the argument against repeated collisions is that after a collision of a particle pair the particle velocities are directed in a way that physically a second collision of the same pair is not possible. However, an analogous argument is valid for particle velocities of any pair before checking it for a collision. More precisely, if one imagines a gas in equilibrium, the above described situation is true in mean for the first collisions of the half of possible pairs. So, it can be shown that the problem with repeated collisions in the DSMC collision schemes is rather mathematical than physical and it can be explained considering the local property of the collision integral in the Boltzmann equation. At any instant t, the collision integral is defined in a single point x. From physical viewpoint, if one considers a local set of particles in $\boldsymbol{x}$ it means that all particles

* Corresponding author.
E-mail address: e.roohi@ferdowsi.um.ac.ir (E. Roohi).

https://doi.org/10.1016/j.compfluid.2017.11.005
0045-7930/

Nomenclature

CF_{th}	theoretical collision frequency at the equilibrium state
CF	numerical collision frequency
CF^*	the ratio of numerical collision frequency to the theoretical value
d	molecular diameter
Δx	collision cell size
Δt	time step
Δt_w	wall time sampling period
ΔT_w	walls difference temperature
ε^i	molecular energy of incident particle to the wall
ε^r	molecular energy of reflected particle from the wall
F_n	ratio of the number of real molecules to the simulated particles
f	probability distribution function
K_B	Boltzmann constant
L	wall spacing in Fourier flow
λ	molecular mean free path
M	molecular mass
MCS	mean collision separation
N_{pair}	number of pair selections
N_{col}	number of collisions in cell
N_{dup}	number of duplicate collisions in cell
N_c	number of cells
N_m	instantaneous number of particles in cell
$\langle N_m \rangle$	time-averaged number of particles in cell
n	number density
p_{ij}	collision probability
ω	viscosity-temperature exponent
q^*	normalized heat flux to its converged value
S	surface area
SCR	successive collision ratio
SOF	mean collision separation divided by the mean free path
σ	collision cross section
$(\sigma V_R)_{\max}$	maximum value of the product of collision cross-section and collision pair relative velocities
T_c	cold wall temperature
T_h	hot wall temperature
T_{ref}	reference temperature of gas
T_λ	mean free time
V_R	relative velocity
V_{mp}	most probable speed
$\forall_c$	collision cell volume

are in the vicinity of point x, i.e., their positions are indistinguishable from point x. On another side, the collision process is considered for a very small time interval around instant t so that the pre-collision and post-collision times for all possible collisions in the vicinity of point x are associated with instant t. Hence, mathematically one should not distinguish the moment of particle trajectory converging leading to a collision from the moment of particle trajectory diverging after a collision within a time step dt. Thus, any collision depends only on the relative velocity magnitude but not on its sign. In DSMC simulations, a cell with a size of dx around x is considered instead of point x, and it is accepted that it represents approximately the solution in point x. Similarly, the time interval dt around instant t is associated with t and one should not distinguish the post-collision from pre-collision velocities of the particles found in the considered cell. Thus, the argument for avoiding repeated collisions because they are unphysical does not discover correctly the reason for the computational error introduced by repeated collisions in the DSMC calculations. A proper explanation of the effect of repeated collisions is given in the paper [5]. According to Stefanov [5], the multiple repeated elastic collisions of a pair in a cell have the effect of only one collision of that pair on collision process. This statement is true for both variable hard sphere (VHS) and variable soft sphere (VSS) models in case of elastic collisions because both models keep same the magnitude of relative velocity of the colliding pair. For inelastic interactions of polyatomic molecules, the effect of repeated collisions is not investigated, but some collision rate reduction coming from the translational degrees of freedom should also be evident. Thus, the repeated collisions of a pair lead to a reduced local collision rate. Probability analysis of repeated collisions of the NTC scheme given in Ref. [5] showed that repeated collisions increase quickly when the number of particles in cells decreases, and a dominated part of repeated collisions is due to pairs with larger relative velocities, i.e., the probability of repeated collisions is of order $O(P_{ij}/N_m)$, where P_{ij} is the NTC collision probability, and N_m is the number of particles per cell. The solution to the repeated collision problem seems simple – one just has to avoid the repeated collisions directly [6]. However, as it will be shown in the sequel of this paper (Section 3.2), the avoidance of repeated collisions in the NTC scheme has another adverse effect that appears when the number of particles in cells is not sufficient.

There are a few studies focused on the repeated collisions in the DSMC scheme. Shevyrin et al. [7] investigated the influence of repeated collisions on the deviation of the DSMC results from the solution of the Boltzmann equation for heat transfer between two parallel plates and Couette flow. Considering the distributions for macroscopic properties (density, temperature, velocity, heat flux), they showed that the fraction of repeated collisions is a reliable indicator of deviation of simulation results from the solution of the Boltzmann equation.

Bird proposed a new version of the DSMC algorithm with improvements in most of the procedures [6,8]. In the improved NTC algorithm, the problem with the unrealized potential collisions between close particles situated in a cell was resolved by using a deterministic algorithm for finding collision partners. However, the realization of repeated collisions remained a source of stochastic error unless they are explicitly avoided. Bird stated that lower values of separation of free paths (SOF), which is defined as a ratio of mean collision separation to mean free path, largely self-validates the accuracy of DSMC solutions [6]. However, it should be mentioned that this is a necessary but not a sufficient condition. So, it should be noted that low SOF does not always guarantee a correct solution if it is not accompanied with avoiding of repeated collision between particles [9,10]. As a remedy for this problem as well for other problems associated with the NTC scheme such as the so called “reminder” problem, i.e., non-integer reminder when the number of selected particle pairs is calculated in the NTC formula, it is suggested to use 7–10 particles per collision cell. In the relaxation to equilibrium test case, Bird reported that the duplicate collisions were about one percent of the total collisions when there were about ten molecules per collision cell. With Decreasing further the number of molecules per cell the number of repeated collisions increases to two percent at four molecules per cell. Without suppressing duplicate collisions, the collision rate increases by about 0.05% and the agreement with the theoretical equilibrium rate is still satisfactory when there are ten or more simulated particles per collision cell. In this case, the duplicated collisions typically reduced the effective collision rate by about 1% [6]. However, it should be noted that the effect of repeated collision should be investigated for sensitive parameters in complex test cases in more details. The suggested remedy of repeated collisions in the NTC that is directly avoiding them, which means that one introduces a

condition leading to a non-uniform distribution of selection probabilities because for the first chosen pair one chooses randomly among $N(N-1)/2$ pairs of particles but the second choice is performed from among $N(N-1)/2-1$ pairs of particles etc. The effect is stronger if one keeps this direct collision control condition within successive time steps. Evidently, this error is minor for a large number of particles, but it is of considerable importance if there are a few particles per cell [5,11].

Here, we provide a detailed investigation of the behavior of the standard NTC scheme in the presence or absence of "successively repeated collisions." The consequences of successively repeated collisions on the heat flux prediction of the Fourier heat transfer problem are evaluated in the early slip regime, investigating the collisional and statistical parameters, as well as the heat flux values predicted at presence or absence of duplicate collisions in the classical NTC scheme. The effects of different parameters such as number of particles, number of cells, time step, and level of duplicated collisions on the heat flux of Fourier problem are examined in details.

2. NTC collision scheme

In the standard NTC scheme, the number of collision pairs, N_{pair} in the cell is calculated as [1]:

$$N_{pair} = \frac{1}{2} F_n N_m \langle N_m \rangle (\sigma V_R)_{\max} \frac{\Delta t}{\forall_c} \tag{1}$$

where both instantaneous, N_m, and average number, $\langle N_m \rangle$, of particles in the cell are employed for the determination of N_{pair}. The recent variant of the NTC [6,8] uses the term $N_m(N_m-1)$ instead $N_m\langle N_m\rangle$ in Eq. (1), i.e.,

$$N_{pair} = \frac{1}{2} F_n N_m (N_m - 1)(\sigma V_R)_{\max} \frac{\Delta t}{\forall_c} \tag{2}$$

In the new relation (2) is taken into account the Poisson distribution property leading to equality $\langle N_c\ (N_c-1)\rangle = < N_c >^2$, which was pointed out by Yanitsky [12] then reemphasized and utilized in Eq. (1) by Stefanov [13], and also presented by Bird in [6,8].

Once selected, the particle pair is tested for the collision by using the acceptance-rejection procedure. The acceptance-rejection logic is set up on a probabilistic concept. For a chosen pair $1 \le (i, j) \le N_m$, the collision occurs if the collision probability becomes greater than a random number between 0 and 1 as:

$$p_{ij} = \frac{(\sigma V_R)_{ij}}{(\sigma V_R)_{\max}} \ge Ranf \tag{3}$$

Considering a grid with a small number of particles per cell, the conditions for accurate simulation using the NTC collision scheme are violated frequently because the relative velocities of the few particle pairs in a cell form a strongly degenerated probability distribution function. This leads to an unacceptable increase in the number of successively repeated collisions in cells. The post-collision velocities obtained as a result of using n successively repeated elastic collisions are statistically distributed in the same way as if they are achieved by the realization of only one collision of the chosen pair [5]. As a consequence, the major effect of the NTC simulation with a small number of particles per cell is a reduction in the local collision frequency, which converges to the Boltzmann collision frequency only for a sufficient number of particles per cell [5].

In the standard NTC scheme, the second particle is selected randomly without extra consideration. But in the scheme avoiding repeated collision, an additional condition is taken into account: the second particle should differ from the last particle, which hit the first before. Here is assumed that a repeated collision means that the same pair of particles experiences collisions in one or several successive time steps without occurrence of collisions with other particles. Based on that, whenever a collision occurs between two particles, the particles are allowed to collide again with each other if at least one of them collides to a third particle or collides with a solid boundary. Otherwise, a new collision of them is not permitted again during the simulation.

The hypothesis of molecular chaos assumed in the derivation of the Boltzmann equation is valid if the probability of repeated collisions is negligibly small [7,11]. Otherwise, statistical correlations will be presented in the solutions. Thus, the occurrence of the repeated collisions is a source of stochastic errors in the NTC scheme.

In previous works, avoiding duplicated collisions were performed via a list of partners of the last n collisions made for each molecule. Hence, the collision of molecules A and B was considered as repeated if the list of molecule A contains molecule B and the list of molecule B contains molecule A [7]. The parameter n is usually selected by the user. In the current work, we set $n = 1$ [14] to evaluate the effect of avoiding the recollision of the last collision partners for each molecule in all simulation cases considered in this study. After reflecting each molecule from a surface, the list for that molecule is reset.

Different collisional parameters were considered to examine the effect of avoiding duplicated collision in the Fourier problem, i.e. heat flux, collision frequency, the ratio of accepted collisions to selected pairs, repeated collisions ratio, and mean collision separation. The net heat flux to the wall is calculated from the net energy exchanged with the wall by the incident and reflected molecules as follows [1]:

$$q_w = \frac{\sum \varepsilon^i - \sum \varepsilon^r}{\Delta t_w \,.\, S} \tag{4}$$

The equilibrium collision rate per molecule is given theoretically (CF_{th}) by [1]:

$$CF_{th} = 4nd^2 \left(\frac{\pi K_B T_{ref}}{m}\right)^{0.5} \left(\frac{T}{T_{ref}}\right)^{1-\omega} \tag{5}$$

CF represents the numerical collision frequency that is calculated by the division of the number of collisions in each cell N_{col} on the execution time, and half of the mean particle numbers per cell as follows:

$$CF = \frac{2N_{col}}{\langle N_m \rangle Time} \tag{6}$$

The parameter CF^* is the ratio of the numerical CF to its theoretical value—that is the equilibrium state—it should have a magnitude close to unity. The heat transfer problem considered in this investigation is under conditions close to linear assumption corresponded to small relative temperature gradient values. This allows using CF^* as a meaningful criterion for accuracy check.

The level of duplicated collisions in each cell is called as "Successive Collisions Ratio (SCR)":

$$SCR = \frac{N_{dup}}{N_{col}} \tag{7}$$

The normalized mean collision separation is as:

$$SOF = \frac{MCS}{\lambda}, \tag{8}$$

where λ is the local mean free path in the cell. The values of SOF much smaller than the unity reflects a suitable collision quality [6]. Probability distribution functions for relative velocity of collision pairs, the number of collisions, and the number of particles in the cell are considered in this paper. The probability distribution function of an arbitrary parameter ϑ is defined as f_ϑ, where:

$$\int_{-\infty}^{+\infty} f_\vartheta \, d\vartheta = 1 \tag{9}$$

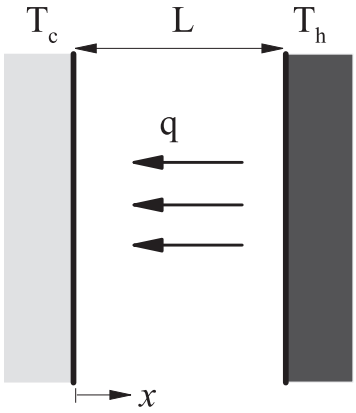

Fig. 1. Geometry of the Fourier flow.

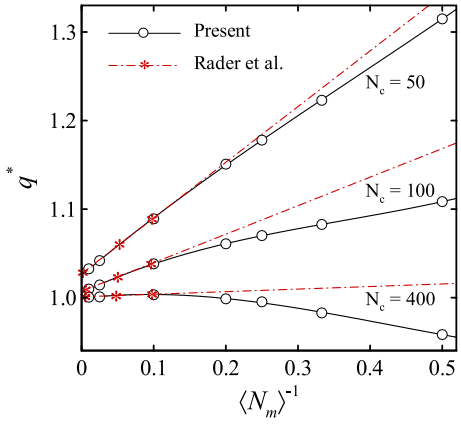

Fig. 2. Heat flux values obtained by the classic NTC scheme; considering different number of particles per cell and different cell numbers; $\Delta t = 0.1\,t_\lambda$.

3. Results and discussion

The Fourier problem, i.e., the heat transfer through a rarefied gas confined between two infinite parallel walls separated by a distance L at different temperatures, as shown in Fig. 1, is considered here for evaluation of the repeated collision effects. Hard sphere argon gas ($m = 6.63 \times 10^{-26}$ kg, $d = 3.658 \times 10^{-10}$ m, $\omega = 0.5$) at the average temperature of 273.15 K and pressure of 266.6 Pa is considered. The wall is located at $L = 1$ mm, cold and hot walls are at $T_c = T_{ref} - \Delta T_w/2$ and $T_h = T_{ref} + \Delta T_w/2$, where $\Delta T_w = 100$ K. Based on this condition, the plate distances is approximately 42 times of the average mean free path, i.e., Kn = 0.024. The simulation test case has been selected based on the work of Gallis et al. [15–17], and our results were compared with their NTC results. The converged value of the heat flux for this simulation is reported as 1512 W/m^2 [17–19]. In all simulations, collisional cell size and time step are set in such a way that to be much smaller than the local mean free path (λ) and mean collision time, respectively.

3.1. Classical NTC scheme (without a procedure of avoiding repeated collisions)

In the current section, we investigate the effect of repeated collisions on the standard NTC scheme using Bird's DSMC1 code. Compared to Ref. [17], we report simulations with a smaller number of particles per each cell. Fig. 2 shows the variation of heat flux versus the number of particles in cell for different cell numbers (N_c). The results are compared with those of Rader et al. [17] at a time step of 7 ns which is equivalent to $0.1 \times t_\lambda$. For $\langle N_m \rangle$ greater than 10, there is a linear relation between heat flux and $\langle N_m \rangle^{-1}$. Operator $\langle\rangle$ means the average values in the computational domain. Decreasing $\langle N_m \rangle$ below 10 leads to an underestimation of the predicted heat flux from the linear relation. Dashed-dotted lines indicate linear extrapolation based on Rader et al. results reported for large $\langle N_m \rangle$. As it is seen, a decrease in the cell number leads to an increase in the predicted heat flux. The increase in the number of particles increases heat flux for cases of $N_c = 50$, 100, but it decreases heat flux for case $N_c = 400$. We justify this behavior in the rest of the paper.

Fig. 3 demonstrates the distribution of *SCR* values for various $\langle N_m \rangle$ and N_c values. Using a lower number of particles leads to a higher rate of repeated collisions. It is evident that the fewer is the number of particles, the lower are the choices for selection of collision partner. Moreover, at the same time step, *SCR* is higher for larger cell sizes, i.e., smaller N_c. Larger cell sizes accompanied with a small time step permits the particles to remain a longer time in the same cell, which increases the probability of repeated collisions. Fig. 3-a shows that SCR could increase to 15–21% if a coarse cell ($N_c = 50$) and a small number of particles per cell ($\langle N_m \rangle = 2$) is utilized. The figure shows that in the case of $N_c = 50$, there is an increase in the *SCR* from the cold wall towards the hot one. This is in accordance with the theoretical probability evaluation of the repeated collision given by Stefanov [5], i.e., repeated collision are of an order of $O(P_{ij}/N_c)$. As most of the high-speed particles are accumulated near the hot wall, and gas density is lower there, and repeated collisions are more probable near the hot wall.

Fig. 4 reports the distribution of collision frequency ratio for a various number of particles per cell and cell numbers of 50 and 400. Collision frequency ratio is higher than unity for lower particle and smaller cell numbers. According to the figure, CF^* depends on the number of particles even at a fixed cell size. In the case of small cell and particle numbers, CF^* increases from cold towards the hot wall. This is due to the appearance of the particle number in the denominator of Eq. (6). Our results show that there are less number of particles near the hot side of the geometry, see Fig. 5. Moreover, the slope of CF^* is higher for the lower number of cells.

Probability distribution functions for the number of particles and collision number are shown in Fig. 5 for $N_c = 50$, $\langle N_m \rangle = 5$, $\Delta t = 0.1\,t_\lambda$. The results are obtained for three cells in the computational domain, i.e. adjacent to the cold wall, middle, and adjacent to the hot wall. The symbols correspond to DSMC simulations, and lines indicate analytical Poisson distribution given for a phenomenon with N occurrence as follows:

$$P(N) = \frac{\langle N \rangle^N}{N!} e^{-\langle N \rangle} \tag{10}$$

According to Fig. 5, the probability function for the number of particles and collision number in a cell suitably follow the Poisson distribution. It is also observed that the most probable values of particle number and collision number are higher for the adjacent cell to the cold wall. The accumulation of particles near the cold wall follows the density gradient. In a steady state condition, the temperature and density gradients have opposite signs in order to fulfill the equation of state. The distribution of number of collisions also shows that number of collision is smaller on the hot side. This behavior is due to lower number of particles there.

Fig. 6 shows the probability function distributions for relative velocity of accepted collision pairs. For a lower number of particles, i.e., $\langle N_m \rangle = 2$ the probability of the most probable value of the relative velocity is slightly lower, while there is a slightly larger probability for higher relative velocities. This means that the chance of acceptance of collision pair is slightly higher at a lower number of particles. This could be a partial reason of higher CF^* at lower $\langle N_m \rangle$.

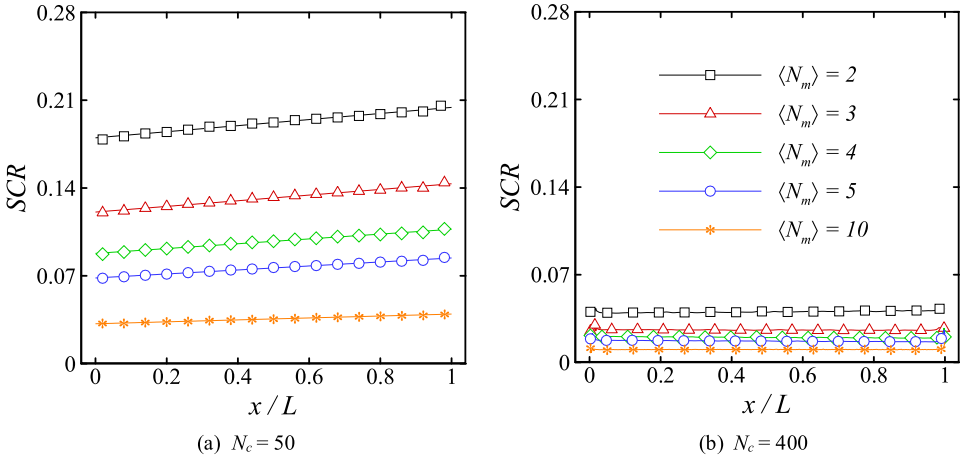

Fig. 3. Distributions for successive repeated collisions ratio; $\Delta t = 0.1\ t_\lambda$.

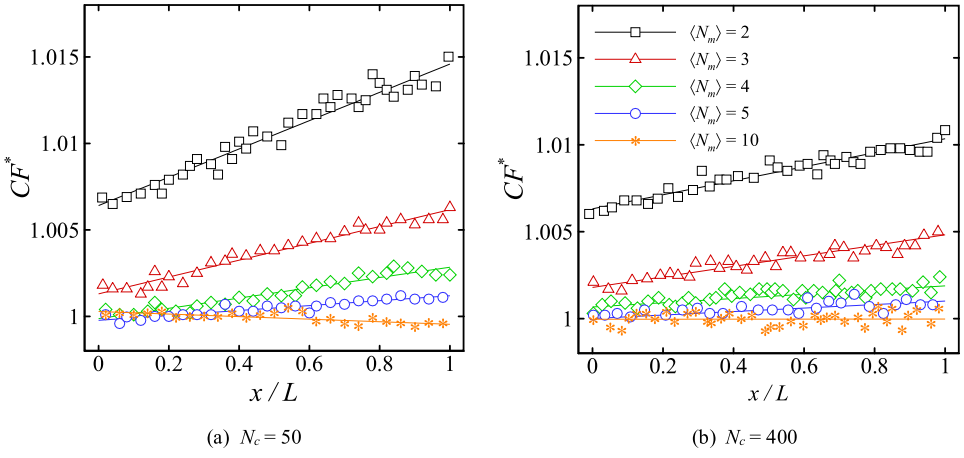

Fig. 4. Distributions of collision frequency ratio; $\Delta t = 0.1\ t_\lambda$.

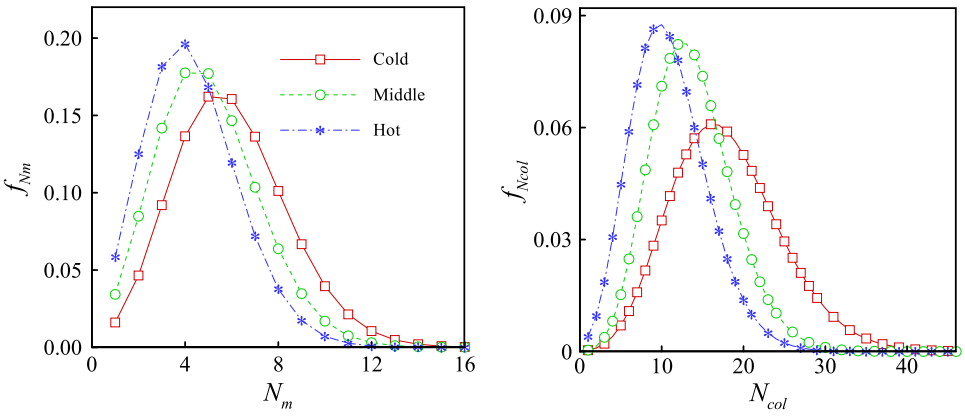

Fig. 5. Probability distribution functions for number of particles and number of collisions in cells adjacent to hot wall, middle and adjacent to cold wall; Poisson distributions (lines) and DSMC simulations (symbols); $N_c = 50$, $\langle N_m \rangle = 5$, $\Delta t = 0.1\ t_\lambda$.

Fig. 7 investigates the effect of number of particles per cell on different parameters, i.e., normalized heat flux, mean collision separation, fraction of repeated collision, and collision frequency ratio. The investigation is performed for various cell numbers of 50, 100, and 400. Normalized heat flux decreases and approaches to unity as the number of particles increases in $N_c = 50$ and $N_c = 100$ cases. In the case of $N_c = 400$, the normalized heat flux increases as $\langle N_m \rangle$ increases up to 10, after that it decreases slightly and approaches to unity. This observation indicates that the heat flux exhibits a mixed behavior with respect to the $\langle N_m \rangle$ at a sufficiently large number of cells, i.e., it overpredicts the limiting value at a lower $\langle N_m \rangle$ and underpredicts at a higher $\langle N_m \rangle$. For detection of the reason for this behavior, the variation of the other collisional parameters reported in Fig. 7 should be considered.

Theoretically, the mean separation between two random points in a unit-size 1-D cell is 0.333333 [15]. However, mean collision

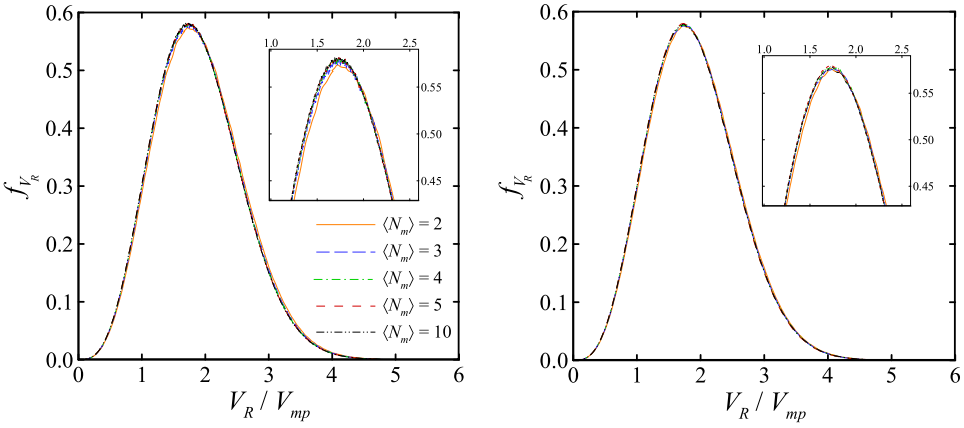

(a) $N_c = 50$ (b) $N_c = 400$

Fig. 6. Probability distribution functions for relative velocity of collision pairs; $\Delta t = 0.1\, t_\lambda$.

separation changes with reducing $\langle N_m \rangle$ due to the repeated collision effects. Variations of non-dimensional mean collision separation (*SOF*) versus $\langle N_m \rangle$ are shown in Fig. 7. It is well observed that *SOF* increases as $\langle N_m \rangle$ decreases. However, the effect of $\langle N_m \rangle$ is negligible for $N_c = 400$. This indicates that at a sufficiently high number of cells, *SOF* is approximately independent on $\langle N_m \rangle$. Decreasing number of particles down to $\langle N_m \rangle = 2$ leads to an additional 6%, 4%, and 0.15% growth in *SOF* (with respect to the expected theoretical value corresponding to a large number of particles per cell, i.e., case with $\langle N_m \rangle = 10^2$) for $N_c = 50$, 100, and 400, respectively. Therefore, lower values of $\langle N_m \rangle$ and N_c increase *SOF*. Increasing *SOF* means that collisions have been performed by farther particles. This leads to an overprediction of the heat flux.

Decreasing $\langle N_m \rangle$ leads to increase in successive (repeated) collision ratio (*SCR*) up to 20%, 13%, and 4% for $N_c = 50$, 100, and 400, respectively. Fig. 7 shows that *SCR* continuously increases as $\langle N_m \rangle$ decreases. The repeated collisions constitute a considerable portion of collisions at a lower number of particles. This leads to a wrong heat transfer prediction at a lower $\langle N_m \rangle$. Fig. 7 illustrates that as the number of particles decreases up to 2, collision frequency grows 1.1%, 1.1% and 0.8% with respect to the theoretical value in Eq (6), for $N_c = 50$, 100, and 400, respectively. According to Fig. 7, collision frequency ratio mainly depends on the number of particles, and it significantly increases if there are a few particles per cell.

It was observed in Fig. 2 that the heat flux has a mixed behavior for the case with $N_c = 400$, while there are the same *CF* variations (with respect to the $\langle N_m \rangle$) for different cell numbers. Therefore, the origin of the diverse behavior of heat flux in this case is the competition between *SOF* effects and *SCR* effects due to variations of particle numbers in the cell. As $\langle N_m \rangle$ decreases, the heat flux goes up due to the collisions between more distant particles and at the same time tends to decrease due to the ineffective collisions resulting from successively repeated collisions. In the cases of $N_c = 50$ and 100, the additive effect of collisions between farther particles is dominant in all range of $\langle N_m \rangle$ variations, and heat flux increases due to the decrease of $\langle N_m \rangle$. But in the case of a sufficient number of cells ($N_c = 400$), the additive effect of farther particle collisions is dominant up to $\langle N_m \rangle = 10$, thereafter that subtractive effect of repeated collisions becomes dominant. Therefore, in the case of $N_c = 400$, the heat flux first increases as $\langle N_m \rangle$ decreases up to $\langle N_m \rangle = 10$ and after that decreases with the further reduction of $\langle N_m \rangle$.

Fig. 8 illustrates the effect of mean collision separation and repeated collisions on the resulted heat flux for three considered cell sizes. As it is seen, *SOF* strongly affects the heat flux in a such way that lower *SOF* values leads to a normalized heat flux closer to unity. However, there are variations in heat flux at approximately constant *SOF* which is due to the variations in *SCR* and CF^* values. The heat flux increases with the *SCR* decrease in cases of $N_c = 400$, while it decreases with the *SCR* decrease for other cell sizes. Actually, in the cases of $N_c = 50$ and 100, the heat flux increases due to the increase of *CF*. In general, one could conclude that lower $\langle N_m \rangle$ values lead to higher *SCR*, which decreases the effective heat exchange, and a higher *CF*, which increases the heat flux. The competition between these effects leads to mixed behavior of obtained heat flux in Fourier problem versus the number of particles. In the case of $N_c = 50$ and 100, the effect of *CF* is dominant. But in the presence of a suitable cell size, the effect of *SCR* is dominant in the realization of heat flux behavior versus the number of particles.

Fig. 9 shows the variations of heat flux obtained by classical NTC method with respect to the number of particles per cell for different cell numbers and time steps. The results are compared with those of Rader et al. [17] (solid lines) obtained for $\Delta t = 0.1 T_\lambda$. As it is seen, with the decrease in the number of particles for all cell numbers and time steps, the additive effect of farther-particles collision is dominant against the subtractive effect of the repetitive collisions on the heat flux. Hence, heat flux increases as the number of particles per cell decreases. The time step increment has an additive effect on heat flux. It will be discussed in following figures. Fig. 10 repeats the calculations performed in Fig. 9 for the NTC scheme using Eq. (2) instead of Eq. (1). The figure indicates that where an appropriate time step is applied, heat flux is reduced if Eq. (2) is used.

Fig. 11 reports the variations of average repeated collision ratio SCR for different cell numbers, particles per cell, and time steps. As expected, the decrease in the number of particles and number of cells leads to an increase in the number of duplicated collisions. An interesting result is obtained considering the time step variation. In the NTC scheme, the decrease of time step leads to a reduction of the maximum number of selected collision pairs in a collision cell. One should also expect a reduction in the fraction of repeated collisions. However, for a given particle pair the collision probability is determined by the acceptance-rejection rule with the probability given by Eq. (3) that does not depend on time step. Thus, the chance of a repeated collision of a twice chosen pair in the NTC algorithm does not decrease with the reduction of the time step. This explains the similar levels of repeated collisions shown in (a)–(c).

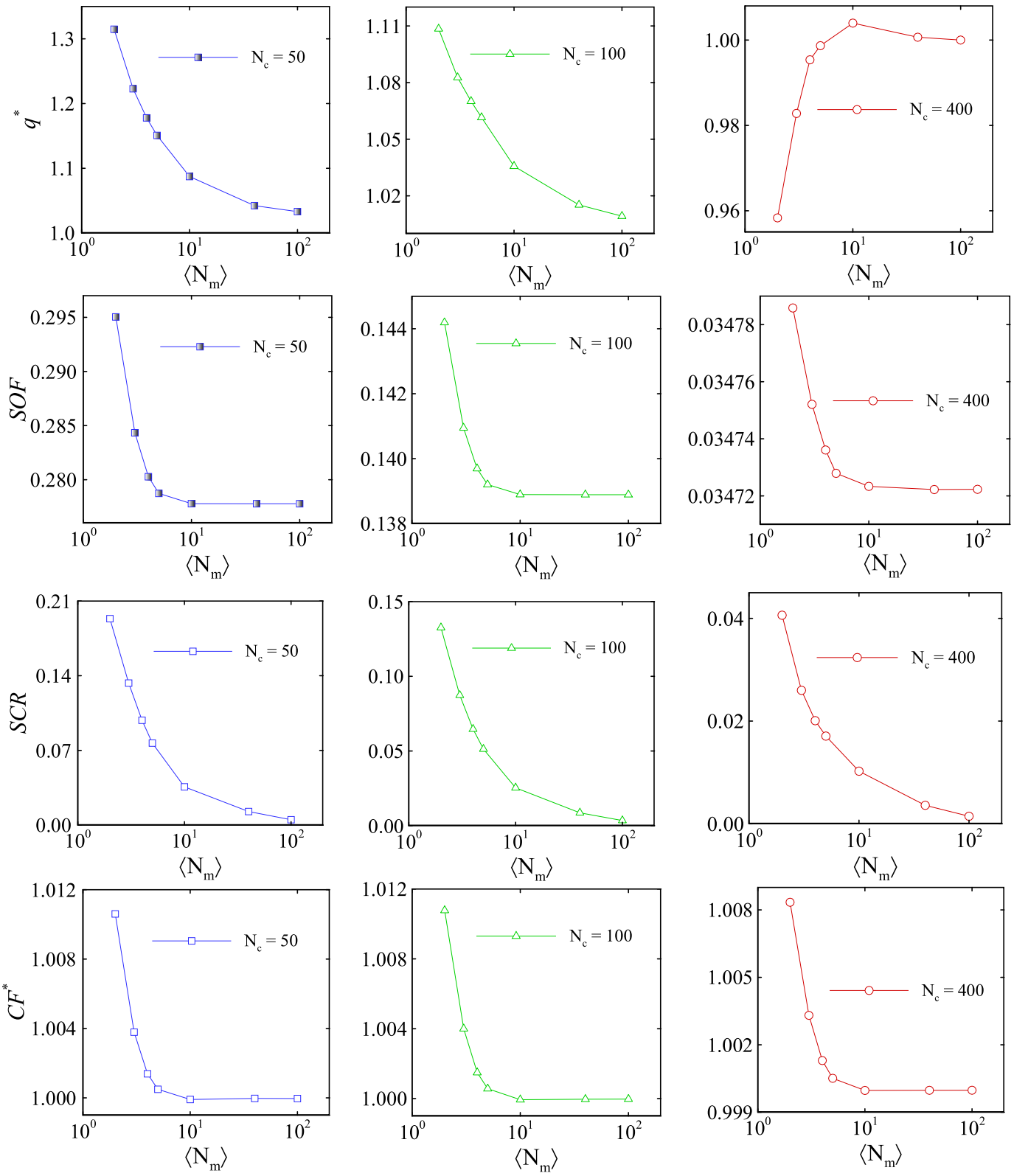

Fig. 7. Number of particles effects on heat flux, mean collision separation, duplicate collision ratio, and collision frequency; $\Delta t = 0.1\ t_\lambda$.

3.2. Avoiding repeated collisions

To investigate the consequences of avoiding repeated collisions, we reconsider the simulation test case reported in Fig. 9 for the NTC scheme but with no possibility of successively repeated collision in the Bird's DSMC1 code. We directly avoided repeated collision using the procedure already discussed in the paper and employed in DS2V code [6]. The heat flux results are demonstrated in Fig. 12. Comparison between Figs. 9 and 12 indicates that the avoidance of repeated collisions considerably reduces the

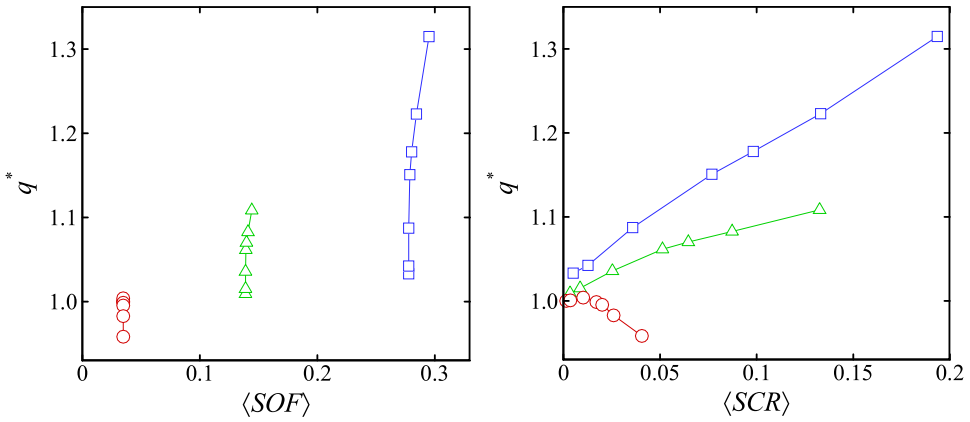

Fig. 8. Effect of mean collision separation and duplicate collision ratio on heat flux; $\Delta t = 0.1\ t_\lambda$, rectangle symbol: $N_c = 50$, triangle symbol: $N_c = 100$, circle symbol: $N_c = 400$.

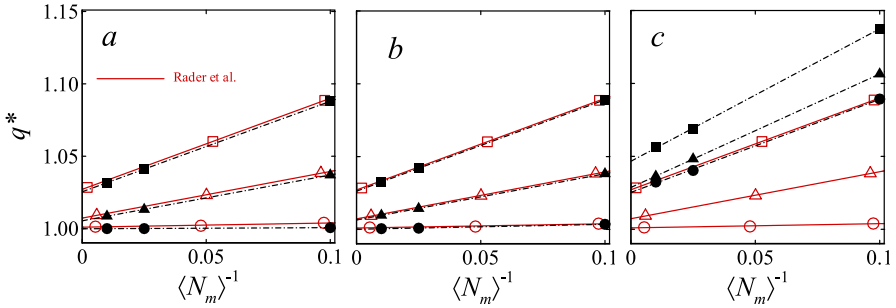

Fig. 9. Heat flux values obtained from the classic NTC scheme; considering different number of particles, cell numbers of 50 (□), 100 (△), 400 (○), and time steps of (a) $\Delta t = 0.01\ t_\lambda$, (b) $\Delta t = 0.1\ t_\lambda$, and (c) $\Delta t = t_\lambda$.

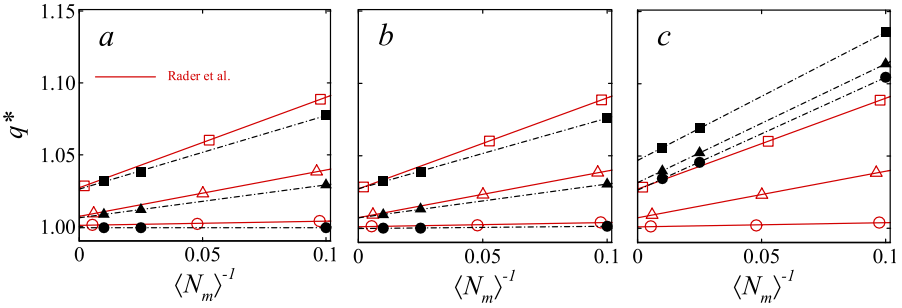

Fig. 10. Heat flux values obtained from the classic NTC scheme but using Eq. (2); considering different number of particles, cell numbers of 50 (□), 100 (△), 400 (○), and time steps of (a) $\Delta t = 0.01\ t_\lambda$, (b) $\Delta t = 0.1\ t_\lambda$, and (c) $\Delta t = t_\lambda$.

predicted heat flux. This leads to a closer estimation of the heat flux especially in the case of a higher cell number and lower time steps (dashed-dotted lines and filled circles in Fig. 12-a,b). In the cases with $\Delta t = 0.1 T_\lambda$, $N_c = 400$, the heat flux decreases as $\langle N_m \rangle$ decreases. This is similar to the behavior detected in Fig. 2 for $N_c = 400$ and $\langle N_m \rangle$ less than 10.

To highlight the effect of duplicated collisions, we considered a case with $N_c = 50$, $\langle N_m \rangle = 2$ where a high rate of duplicated collision ratio was observed. From probability distribution functions for relative velocity of colliding particles and number of collisions, it is found out that the avoidance of duplicate collisions decreases the mean relative velocity of the collided pairs and hence reduces the probability for acceptance of the collision. This observation is in accordance with the probability analysis of Ref. [5] which showed that repeated collisions are most probable for particles with higher relative velocity. Therefore, an average number of collisions diminishes. Also, according to Eq. (3), the collision probability is lower for lower values of V_R. As reported by Gallis et al. [15], the theoretical average mean collision separation in classical NTC scheme, i.e., the average distance between two colliding particles, is equal to 1/3 times of the collisional cell size. However, in the absence of the duplicated collisions, it increases by 5% in the present case. This higher *MCS* values leads to farther-particles collisions. These farther-particle collisions detected in Fig. 13 could be the reason for a higher heat flux prediction reported in Fig. 8.

Fig. 14 shows the variations of normalized heat flux with the simulation time step for different cell numbers and numbers of particles at absence of duplicated collisions. The heat flux variation at low time steps is negligible, but it is significant at large time steps increasing dramatically the heat flux. The same trends were observed by the classical NTC. In the absence of duplicated collisions, increase in the heat flux due to higher time steps is less compared to the case with duplicated collisions. It is due to this fact that collision frequency significantly decreases at high time steps in the absence of duplicated collisions; See Fig. 15. Meanwhile, in the case of classical NTC, the *CF* approximately remains equal to theoretical value. The main reason for the reduction of *CF*

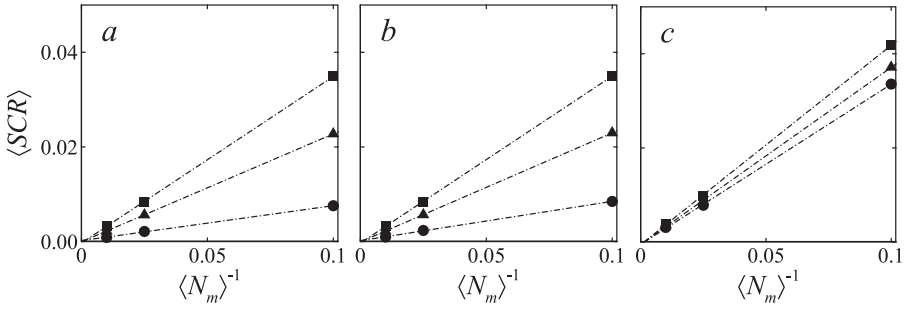

Fig. 11. Fraction of repeated collisions SCR in NTC scheme for different numbers of cells, i.e. 50 (□), 100 (△), 400 (○), and time steps of (a) $\Delta t = 0.01\ t_\lambda$, (b) $\Delta t = 0.1\ t_\lambda$, and (c) $\Delta t = t_\lambda$.

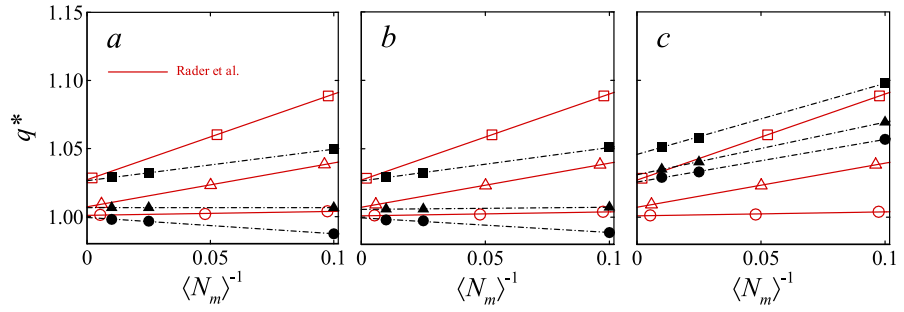

Fig. 12. Heat flux values obtained from the NTC scheme avoiding the successively repeated collisions (dashed lines) considering a different number of particles, cell numbers of 50 (□), 100 (△), 400 (○), and time steps of (a) $\Delta t = 0.01\ t_\lambda$, (b) $\Delta t = 0.1\ t_\lambda$, and (c) $\Delta t = t_\lambda$.

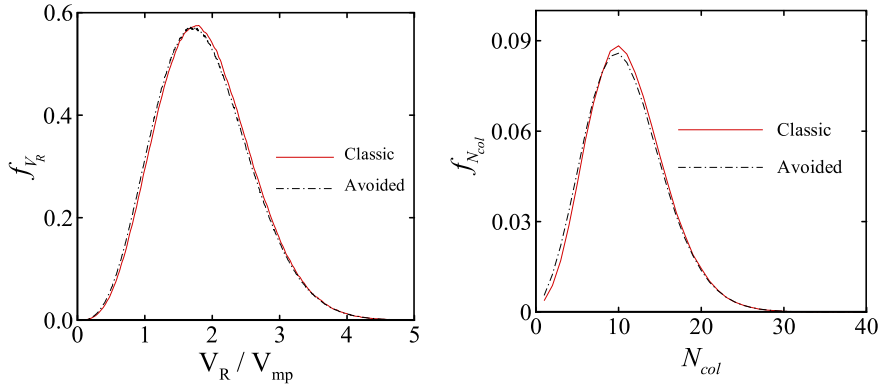

Fig. 13. Effects of repetitive collisions avoidance in NTC scheme on relative velocities, number of collisions, mean collision separation, and accepted collisions ratio.

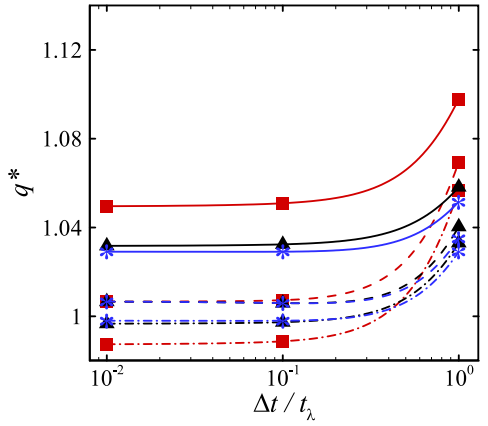

Fig. 14. Variation of heat flux values versus time step for NTC scheme avoiding the successively repeated collisions; considering different cell numbers of 50 (solid lines), 100 (dashed lines), 400 (dashed-dotted lines) and particles per cell of 10 (□), 40 (△), 100 (*).

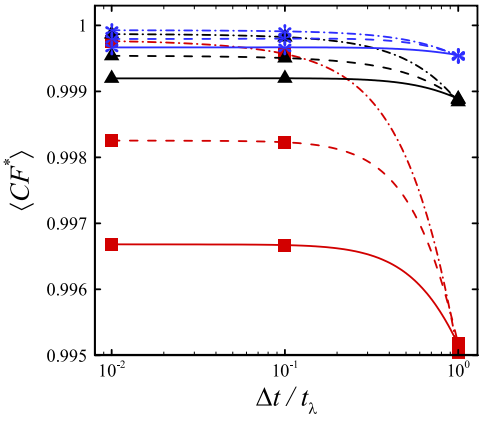

Fig. 15. Variation of collision frequency ratio versus time step for NTC scheme avoiding the successively repeated collisions; considering different cell numbers of 50 (solid lines), 100 (dashed lines), 400 (dashed-dotted lines) and particles per cell of 10 (□), 40 (△), 100 (*).

in the absence of duplicate collision is lower relative velocities of collision pairs as discussed in the results shown in Fig. 12.

4. Conclusions

The effects of successive duplicated collisions and their avoidance on the DSMC calculations by using NTC collision scheme were detected and discussed in details in the case of Fourier heat transfer problem. It was shown that in addition to collision separation and collision frequency, the percentage of repeated collisions also plays an essential role in the accuracy of DSMC simulations. Our investigations indicated that the direct avoidance of duplicate collisions decreases the chance of acceptance of collisions of pairs with higher relative velocities. As the NTC probability depends on relative velocity, this prevention reduces the average collision probability, and consequently, decreases the collision frequency. This effect increases critically for the accuracy of heat transfer calculations when the number of particles in a cell decreases to several. Therefore, avoiding successively duplicate collisions in NTC may lead to underprediction of heat flux in simulations with a small number of particles. As shown for the classical NTC scheme, a lower number of particles at fixed cell size leads to a higher collision separation, and consequently, to an increase of the predicted heat flux. However, in fine grid cases, i.e., for sufficiently small collision separation values, a very low number of particles results in a considerable percentage of duplicated collisions. Duplicated collisions have no effective role in the heat transfer as they count as an effective one collision, therefore; heat flux reduces. For higher *SOF* values, the additive effect of farther-molecules collisions prevails the subtractive effect of duplicated collisions and consequently heat flux increases as the total number of particles decreases. This is a mixed behavior of heat flux in the Fourier problem with respect to the particle numbers. This mixed behavior could also be detected in the NTC scheme with avoidance of duplicated collisions. At sufficiently small *SOF* values, the heat flux decreases as the number of particles decreases due to a significant reduction of the collision frequency. At higher *SOF* values, the heat flux increases as the number of particles decreases, however; the slope of heat flux curve is less than that of the standard NTC scheme. The direct prevention of repeated collisions introduces additional errors in the standard NTC scheme when the number of particles per each cell is small. In this case, the collision procedure may check many times the same pair that previously was rejected. Next time the routine can choose the same pair and check it until a collision is realized. Using the direct prevention procedure, a conditional probability with removing from consideration some pairs destroys the correct random choice of pairs and the non-uniformity of selection probability distribution becomes significant. Moreover, the direct prevention of repeated collisions will eventually result in selecting pairs with smaller relative velocities, that have a lower chance for acceptance. The consequence is a deviation from the correct collision probability, defined in the Boltzmann equation, what leads to an incorrect collision frequency, and respectively, to an incorrect heat flux in DSMC calculations using NTC scheme with small number of particles in cells.

Acknowledgments

The authors from the Ferdowsi University of Mashhad would like to acknowledge the financial support provided by the Faculty of Engineering, Ferdowsi University of Mashhad under Grant No. 42970. S.S. acknowledges the financial support provided by the Bulgarian National Science Fund under Grant DN-02/7-2016.

References

[1] Bird GA. Molecular gas dynamics and the direct simulation of gas flows. Oxford: Oxford University Press; 1994.
[2] Ivanov MS, Markelov GN, Gimelshein SF. Statistical simulation of reactive rarefied flows: numerical approach and applications. In: Proceedings of the 7th AIAA/ASME joint thermophysics and heat transfer conference, Albuquerque; 1998.
[3] K.A. Stephani, D.B. Goldstein, and P.L. Varghese, Development of a hybrid DSMC/Navier-Stokes solver with application to the STS-119 boundary layer transition flight experiments, AIAA Paper 2011-0534, 2011.
[4] Stephani KA, Goldstein DB, Varghese PL. Parametric study of hypersonic boundary layer flow over discrete surface roughness using a hybrid DSMC/Navier-Stokes solver. In: Proceedings of the 41st AIAA fluid dynamics conference and exhibit; 2011.
[5] Stefanov SK. On DSMC calculation of rarefied gas flows with small number of particles in cells. SIAM J Sci Comput 2011;33(2):677–702.
[6] Bird GA. The DSMC method. USA: CreateSpace Independent Publishing, Platform; 2013.
[7] Shevyrin AA, Bondar YA, Ivanov MS. Analysis of repeated collisions in the DSMC method. In: Capitelli M, editor. Proceedings of the 24th symposium on rarefied gas dynamics, Melville, NY; 2005. p. 565–70.
[8] Bird GA. Sophisticated DSMC. Notes prepared for a short course at the DSMC07 meeting, Santa Fe, USA; 2007.
[9] Bird GA. Visual DSMC program for two-dimensional and axially symmetric flows, the DS2V program user's guide, Ver. 2.1. Sydney, Australia: G.A.B. Consulting Pty Ltd; 2003.
[10] Bird GA. The DS2V/3V program suite for DSMC calculations. In: 24th international symposium on rarefied gas dynamics, vol. 762. American Institute of Physics; 2005. p. 541–6.
[11] Roohi E, Stefanov S. Collision partner selection schemes in DSMC: from micro/nano flows to hypersonic flows. Phys Rep 2016;656:1–38.
[12] Yanitskiy VE. Operator approach to direct simulation Monte Carlo theory in rarefied gas dynamics. In: Beylich A, editor. Proceedings of the 17th symposium on rarefied gas dynamics. New York: VCH; 1990. p. 770–7.
[13] Stefanov S, Cercignani C. Monte Carlo simulation of Bénard's instability in a rarefied gas. Eur J Mech B Fluids 1992;11(5):543–54.
[14] Johnson RW. The handbook of fluid dynamics. Washington: CRC Press; 2016.
[15] Gallis MA, Torczynski JR, Rader DJ, Bird GA. Convergence behavior of a new DSMC algorithm. J Comput Phys 2009;228(12):4532–48.
[16] Gallis MA, Torczynski JR. Effect of collision-partner selection schemes on the accuracy and efficiency of the direct simulation Monte Carlo method. Int J Numer Methods Fluids 2011;67(8):1057–72.
[17] Rader DJ, Gallis MA, Torczynski JR, Wagner W. Direct simulation Monte Carlo convergence behavior of the hard-sphere-gas thermal conductivity for Fourier heat flow. Phys Fluids 2006;18:077102.
[18] Taheri E, Roohi E, Stefanov S. On the convergence of the Simplified Bernoulli Trial collision scheme in rarefied Fourier flow. Phys Fluids 2017;29(6).
[19] Roohi E, Stefanov S, Shoja-Sani A, Ejraei H. A generalized form of the Bernoulli trial collision scheme in DSMC: derivation and evaluation. J Comput Phys 2018;354C:476–92.